# Lecture 8: Tidal Rectification and Stokes Drift

Chris Garrett

## 1 Introduction

In this lecture, we examine how tidal flow which may be thought to be purely oscillatory can affect the mean flow. In §2 we examine flow separation and in §3 we look at the residual flow over a promontory. In §4 we describe Lagrangian vs. Eulerian motion. We see two arguments for how a clockwise mean flow around George's bank is generated by the tides.

## 2 Flow Separation

First consider the flow over a curved body (see Figure 1). Outside the boundary layer between points A and B, the body causes the streamlines to converge, resulting in acceleration of the outside flow, while the flow decelerates between B and C. Using Bernoulli's law, it can be shown that the accelerating region, the pressure decreases and in the decelerating region, the pressure increases. At the wall, the boundary layer equation is

$$\mu \frac{\partial^2 u}{\partial y^2} = \frac{\partial p}{\partial x}. \tag{1}$$

Thus where the pressure gradient is negative (a "favorable" gradient), $\partial^2 u/\partial y^2$ is also negative, leading to profile A. When the pressure gradient is positive (an "adverse" gradient), $\partial^2 u/\partial y^2$ is positive, leading to profile C. Using continuity, it is seen that the boundary layer grows in the the decelerating zone. The adverse gradient causes deceleration of the region immediately next to the body, as seen in the difference between profiles B and C. If the pressure gradient is sufficiently adverse, the flow can actually reverse at the body as seen in profile D. Where the reverse flow meets the forward flow, the flow will separate from the wall. Turbulent boundary layers are able to withstand the adverse pressure gradient better than a laminar boundary layer because the velocity profile above the body is more uniform and similar to the external flow than in the laminar case. Because of this, the separation point occurs farther along the body and consequently there is a thinner wake, which reduces the drag on the body. [1]

Flow separation can lead to tidal rectification. The next section discusses tidal flow around a promontory and the conditions for separation of tidal flow in the presence of friction.

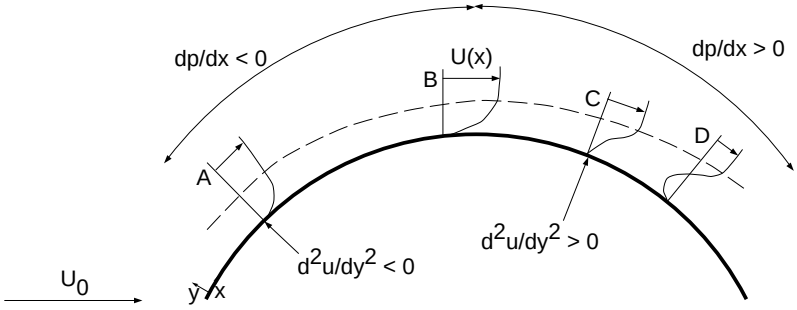


Figure 1: Flow past a curved body. The velocity profiles at various points along the body are shown along with the regions of adverse and favorable pressure gradients.

## 3 Residual circulation at a promontory

Strong tidal currents flow past the Gay Head promontory [2]. Measurements of the currents near the promontory show that there is a net flow away from the promontory. Figure 2 shows a schematic illustration of how this flow is created. When the tide flows past the promontory in one direction, the flow separates, creating an eddy. Then the tide reverses and does the same on the other side of the promontory. The combination of the induced currents creates a residual flow away from the promontory. Geyer and Signell (1990) measured this residual flow and found its average magnitude to be approximately 10% of the tidal flow magnitude. This phenomenon is discussed in the context of flow separation next.

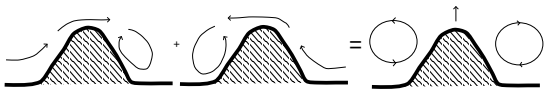

Figure 2: A residual current can be created by tidal flow around a promontory.

Outside the boundary layer next to the promontory, the following governing equation is valid:

$$\frac{\partial u}{\partial t} + u\frac{\partial u}{\partial x} = -g\frac{\partial \zeta}{\partial x} - \frac{C_d u\,|u|}{h}\ , \tag{2}$$

with $x$ following the shape of the promontory. This flow is similar to that described in the previous section, although now friction is present. This has the effect of changing the direct relationship between the pressure gradient and acceleration or deceleration of the flow. Now, even for steady flow, the pressure gradient is balancing both the advective term and the friction term. While in the simple example the pressure gradient directly determined acceleration or deceleration, now the pressure gradient will continue to drive the flow in order to work against the friction. In this case, the flow will remain attached to the promontory and not separate if

$$\frac{C_D U^2}{H} > u\frac{\partial u}{\partial x},$$

where, $U, H$ are the current speed and depth outside a narrow region, near the coast, over which the depth increases from 0 to $H$.

Consider the case of a small promontory (see Figure 3). Flow separation depends on if the pressure gradient is balancing the advective term or the friction term. If the advective term is larger than the friction term then flow separation will occur. The above condition for no separation can be scaled as

$$\frac{C_D U^2}{H} > \frac{U\Delta U}{a} \approx \frac{bU^2}{a^2}.$$

This condition can be restated as

$$\frac{a^2}{b} > \frac{H}{C_D}. \tag{3}$$

Geometry gives

$$a^2 + (R-b)^2 = R^2. \tag{4}$$

For the small promontory, $b \ll a$ so (4) can be rewritten as

$$\frac{a^2}{b} \approx 2R. \tag{5}$$

(3) now reduces to

$$R > \frac{H}{2C_D} \tag{6}$$

for the condition of no separation. For example, using typical values of $H = 20$ m and $C_D = 2.5 \times 10^{-3}$, $R$ must be greater than 4 km to avoid flow separation. Separation is easier if $b \gg a$, or the promontory is much longer than it is wide.

For a given geometry there are controlling factors that dictate if the flow will separate:

$$\frac{b}{a}, \qquad Re_f = \frac{H}{C_D a}, \qquad K_c = \frac{U}{\omega a},$$

where $Re_f$ is a friction Reynolds number, $K_c$ is the Keulegan-Carpenter number, and $\omega$ is the tidal frequency. The ratio of the friction Reynolds number and the Keulegan-Carpenter number is

$$\frac{Re_f}{K_c} = \frac{H\omega}{C_D U} = \frac{\textit{spindown time}}{\textit{period}/2\pi}. \tag{7}$$

Tidal rectification occurs if the flow separates. The above analysis must be expanded for the more realistic situation of a varying depth $H$ and 3D land forms to better evaluate where tidal rectification may occur.

# 4 Lagrangian Motion

There are two basic ways to describe a fluid flow. The Eulerian method, which is often a more natural description for observationalists, describes the flow of a fluid at certain fixed points. Velocity is measured as the flow past a particular point in space and time. The Lagrangian method refers to the flow following a fluid particle. Velocity is measured at

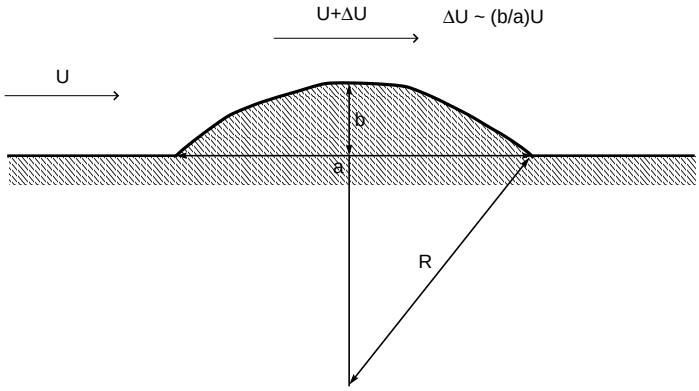


Figure 3: Flow past a small promontory. The promontory causes an increase in the velocity, $\Delta U$ as described in Section 2. For the analysis in the text to be valid, $b \ll a$.

the fluid particle, wherever it is in space and time. Using the subscripts $E$ and $L$ to mean Eulerian and Lagrangian, we have the following relationship between these two velocities for a particular particle at time $t$ which started at position $\mathbf{x}_0$,

$$\mathbf{u}_L(\mathbf{x}_0, t) = \mathbf{u}_E\left(\mathbf{x}_0 + \int_0^t \mathbf{u}_L(\mathbf{x}_0, t')dt', t\right). \tag{8}$$

Note that the expression $\mathbf{x}_0 + \int_0^t \mathbf{u}_L(\mathbf{x}_0, t')dt'$ is simply the position $\mathbf{x}$ of the Lagrangian particle at time $t$.

If we take the average of these velocities in time and expand for small intervals in space, we arrive at the following relationship,

$$\langle \mathbf{u}_L(\mathbf{x}_0, t)\rangle = \langle \mathbf{u}_E(\mathbf{x}_0, t)\rangle + \left\langle \int_0^{t'} \mathbf{u}_L(\mathbf{x}_0, t')dt' \cdot \nabla \mathbf{u}_E(\mathbf{x}_0, t) \right\rangle + \dots \tag{9}$$

$$\approx \langle \mathbf{u}_E(\mathbf{x}_0, t)\rangle + \left\langle \int_0^{t'} \mathbf{u}_E(\mathbf{x}_0, t')dt' \cdot \nabla \mathbf{u}_E(\mathbf{x}_0, t) \right\rangle, \tag{10}$$

where $\langle\cdot\rangle$ is the mean. Assuming $\mathbf{u}_L \approx \mathbf{u}_E$, $\mathbf{u}_L$ in (9) can be replaced by equation $\mathbf{u}_E$ in (10). Dropping higher order terms, we have that the difference between the mean Lagrangian and Eulerian flow is the third term in (10), which is called Stokes drift.

The Stokes drift is like surfing. The more you stay with a wave, the more you drift forward; that is, you stay longer with the forward flow than if were standing still (Eulerian) in which case you would see the forward and backward flow for exactly the same amount of time. This forward drift is Stokes drift.

**An interesting observation.**

If we consider a plane wave, $\mathbf{u}_E = u_0 \cos(kx - \omega t)$ then the Stokes drift becomes

$$\left\langle \int_0^{t'} \mathbf{u}_E(\mathbf{x}_0, t')dt' \cdot \nabla \mathbf{u}_E \right\rangle = \frac{ku_0^2}{\omega} \left\langle \sin^2(kx - \omega t)\right\rangle = \frac{1}{2}\frac{u_0^2}{c},$$

where $c = \omega/k$ is the wave speed. In the non-rotating case, energy is equipartitioned between kinetic and potential energy. In this case,

$$\left\langle \int_0^{t'} \mathbf{u}_E(\mathbf{x}_0, t')dt' \cdot \nabla \mathbf{u}_E \right\rangle = \frac{1}{2}\frac{u_0^2}{c} = \frac{E}{c},$$

where $E$ is energy. For tides, $c$ can be quite large which means that the Stokes drift will be very small.

## 4.1 Example on a Slope: Georges Bank

If we consider a long wavelength tide approaching a bit of topography like Georges Bank in the Gulf of Maine, we can see the relationship between the Lagrangian and Eulerian flows, and the Stokes drift. In this argument, we consider the scale of the topography to be much smaller than the wavelength of the tide so that the wave is in phase all along the bank. Here we are considering an underwater sloping topography rather than a beach since at a beach the waves steepen and break, which are not the dynamics we're interested in. Lastly, the tidal flow makes ellipses due to the oscillation and the Coriolis force. As the wave encounters a sloping bottom, in order to conserve mass the tidal excursion in the horizontal must increase, thereby creating larger tidal ellipses in the shallow water on top of the bank.

### 4.1.1 Hand-Waving Argument

**Kinematic argument.** Using a kinematic argument, we can see that a particle which is advected towards the shallow water by the tide will see a larger tidal ellipse in shallow water, causing it to drift further to the bottom of the figure than it drifts back in the smaller tidal ellipse in deep water. See Figure 4. Thus, the Stokes drift is to the bottom of the figure (counter-clockwise around Georges Bank).

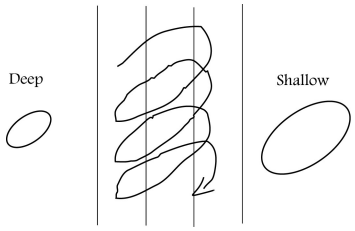


Figure 4: Kinematic argument: Stokes drift of a particle. This figure is a planar view of the underwater topography which is deep on the west and shallow in the east. The parallel vertical lines indicate bottom contours, and the closed ellipses are the tidal ellipses of the $M_2$ tide in deep and shallow water, with a gradient in size of the ellipse between. The curly line over the sloped topography is the path of a particle starting in the deep seas and experiencing the tidal ellipses as it moves to the east.

**Dynamic consideration.** From earlier considerations of drag, we know that it scales as $C_d u^2/h$, where $C_d$ is the drag coefficient, $u$ is velocity and $h$ is depth. This means

that in shallow water, a particle would experience more drag per unit time than in deep water. If we assert that a particle must experience no net force and no net acceleration over a tidal cycle, then the particle must spend less time moving south in shallow water in shallow water than it does in deep water. See Figure 5. Thus Lagrangian flow must be to the north (clockwise around Georges Bank).

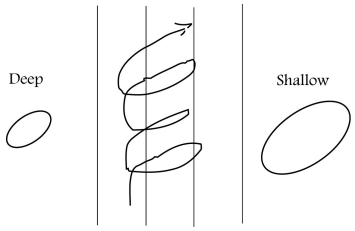


Figure 5: Dynamic consideration: Lagrangian flow of a particle in a tidal cycle. The tidal ellipses and topography are the same as in Figure 4, but the path of a particle using dynamic arguments is to the north rather than the south.

**Eulerian flow.** Since *Lagrangian* = *Eulerian* + *Stokes*, the Eulerian flow must be even stronger to the north (clockwise around Georges Bank) than the Lagrangian flow. Clockwise flow is indeed observed in the mean around Georges Bank.

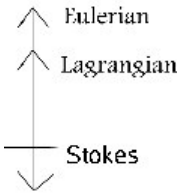


Figure 6: Eulerian flow around Georges Bank as the difference between Lagrangian flow and Stoke's drift.

### 4.1.2 Momentum Argument

This section will describe the tidal rectification around Georges Bank through continuity, Coriolis forces (changing the size of tidal ellipses) and bottom friction. If we consider the momentum equations of a tide encountering a bank averaged over a tidal period, we can solve for the resultant mean flow along the bank. Using 1 subscript to indicate tidal flow, the equations to solve are

$$\left\langle u_1 \frac{\partial u_1}{\partial x} \right\rangle - f \langle v \rangle + g \frac{\partial \langle \zeta \rangle}{\partial x} = 0, \tag{11}$$

$$\left\langle u_1 \frac{\partial v_1}{\partial x} \right\rangle = -\frac{\langle kv \rangle}{H}, \tag{12}$$

where $k = C_d(u^2 + v^2)^{1/2}$ is the frictional drag term at the bottom. We have assumed no mean across bank flow ($\langle u \rangle \approx 0$) and no pressure gradients along the bank ($\partial\zeta/\partial y = 0$).

Solving (12) gives the alongshore current for a given tide, then using $v$ from the solution, (11) gives the across bank pressure gradient. Numerical solutions by Loder using deep and shallow water tidal ellipses and Georges Bank topography confirm the mean clockwise Eulerian flow [3]. He finds that for a tide of frequency $\omega$ with velocities $u_1$, $v_1$ the solutions have frequencies $\omega$, $2\omega$ and higher harmonics as well as the steady, rectified flow.

# 5 Conclusion

In this lecture we have seen how flow which is considered to be purely oscillatory from an Eulerian point of view can create a mean flow, either through interaction with topography or through Stokes drift. The argument for how Stokes drift results from the difference between Eulerian and Lagrangian velocity will be concluded in tomorrow's lecture with a vorticity description.

*Notes by Danielle Wain and Eleanor Williams Frajka*

# References


[1] P. K. Kundu and I. M. Cohen, *Fluid Mechanics, 2ed* (Academic Press, New York, 2001).

[2] W. R. Geyer and R. Signell, "Measurements of tidal flow around a headland with a shipboard acoustic doppler current," J. Geophys. Res. **95(C3)**, 3189 (1990).

[3] J. W. Loder, "Topographic rectification of tidal currents on the sides of Georges Bank," J. Phys. Ocean. 1399 (1980).